Scientific Research Publishing

International Journal of Astronomy and Astrophysics, 2026, 16(4), 339-355
https://www.scirp.org/journal/ijaa
ISSN Online: 2161-4725
ISSN Print: 2161-4717

Study of Warm Dark Matter with the Lyman-α Forest (Part II)

Bruce Hoeneisen

Universidad San Francisco de Quito, Quito, Ecuador
Email: bhoeneisen@usfq.edu.ec

How to cite this paper: Hoeneisen, B. (2026) Study of Warm Dark Matter with the Lyman-α Forest (Part II). *International Journal of Astronomy and Astrophysics*, **16**, 339-355.
https://doi.org/10.4236/ijaa.2026.164020

Received: August 2, 2026
Accepted: October 26, 2026
Published: October 29, 2026

Copyright © 2026 by author(s) and Scientific Research Publishing Inc.
This work is licensed under the Creative Commons Attribution International License (CC BY 4.0).
http://creativecommons.org/licenses/by/4.0/

Open Access

Abstract

Observed quasar light as a function of wavelength shows absorptions due to neutral hydrogen "clouds" along the line-of-sight. This "Lyman-α forest" has a power spectrum that has a cut-off. We study this cut-off. This cut-off may be due to warm dark matter free-streaming in the early universe, or to neutral hydrogen thermal velocity Doppler shift, or both. It is difficult to distinguish between these alternatives. If warm dark matter free-streaming dominates, we obtain the following density power spectrum cut-off wavevector: $k_{\text{fs}} = 5.7 \pm 0.3 \pm 2.0$ Mpc^{-1}. This is a measure of the dark matter "warmness". This result is in agreement with four independent published measurements, and in disagreement with published limits.

Keywords

Lyman-Alpha Forest, Warm Dark Matter, Free Streaming, Dark Matter

1. Introduction

If dark matter is warm, then the comoving density power spectrum $P_{3\text{D}}(k)$ acquires a cut-off at comoving wavevector k_{fs} due to warm dark matter free-streaming in the early universe. The challenge is to measure k_{fs} to determine how warm or cold dark matter is. In the present article we highlight the difficulties of measuring k_{fs} with quasar flux spectra, referred to as the "Lyman-α forest".

Quasar light split into wavelength bins obtains the quasar flux spectra. This flux spectra shows absorption lines corresponding mainly to Lyman-α transitions of proper wavelength $\lambda_\alpha = 1215.67$ Å (followed by isotropic emission) in neutral hydrogen "clouds" along the line-of-sight. These absorption lines are observed to be redshifted: $\lambda = \lambda_\alpha (1+z)$, where z is the redshift of the observed hydrogen "cloud". Let $P_{1\text{D}}(k_z)$ be the observed power spectrum of the quasar flux spectra,

with k_z the wavevector along the line-of-sight (to be explained below). It turns out that this 1-dimesional Lyman-α power spectrum has a cut-off. The purpose of the present study is to try to understand the cause of this cut-off: is it due to i) warm dark matter free-streaming in the early universe, or ii) to baryon thermal effects?

The 3-dimensional density comoving power spectrum $P_{3D}(k)$ acquires a cut-off at comoving wavevector k_{fs} if dark matter is warm. In Part I of this study [1] we assume that the observed Lyman-α power spectra cut-off is due to warm dark matter, and obtain $k_{fs} = 5.0 \pm 2.2$ Mpc^{-1}, in agreement with four independent measurements summarized in Table 3 of [2], but in disagreement with limits summarized in Figure 3 of [3]. The measurements of the dark matter "warmness" k_{fs} are based on density runs of spheroidal dwarf galaxies, from the mass of first generation galaxies, from the stellar mass distributions of spiral galaxies, and from the number density of dwarf galaxies in the local field [2]. In the present article we continue the studies of Part I to try to understand these discrepancies.

Outline: In Section 2, we compare quasar flux power spectra with calculations in 16 bins of redshift z. These power spectra have a cut-off. The calculations assume the observed Lyman-α forest cut-off is due to a density power spectrum cut-off (due to warm dark matter free-streaming in the early universe, Section 3), or to the thermal velocity Doppler shift of neutral hydrogen along the line-of-sight (Section 4). These two phenomena are degenerate: they can not be distinguished with Lyman-α forest observations alone, so independent data is needed. Comments on the observed quasar flux power spectra are presented in Sections 5 and 6. We try to break the degeneracy, *i.e.* find out which cut-off cause is dominant, in Sections 7 and 8. Section 9 presents a summary of data favoring warm or cold dark matter. Conclusions follow. For convenience of non-specialist readers (as myself), mathematical derivations are included in **Appendices A-C**. In **Appendix D**, we compare the present analysis with [4].

2. Data

We analyze Lyman-α power spectra obtained in [5], in 15 bins of redshift from $z = 1.8$ to $z = 4.6$, from three data sources:

- Keck Observatory Database of Ionized Absorption toward Quasars (KODIAQ) Data Release 2 (DR2) ([6]-[8]) observed by HIRES ([9]) on the Keck I telescope.
- The Spectral Quasar Absorption Database (SQUAD) DR1 ([10]) observed by UVES ([11]) on the European Southern Observatory's Very Large Telescope (VLT).
- XQ-100 observed using the X-Shooter spectrograph ([12]) under the European Southern Observatory Large Programme "Quasars and their absorption lines: a legacy survey of the high-redshift universe with VLT/XSHOOTER" ([13]).

In addition, we study Lyman-α power spectra obtained in [14] at redshift $z = 4.2, 4.6$ and 5.0.

The observed Lyman-α power spectra $P_{1D}(k_z)$, obtained in [5] and [14], in 16 redshift bins are presented in **Figures 1-3**. Reference [5] notes that the measurements with $k_z < 0.004$ s/km should be taken with caution because they are subject to large continuum errors, while measurements with $k_z > 0.1$ s/km also need to be taken with caution because they are affected by noise, metal contamination and resolution effects. Several parameters obtained from **Figures 1-3** are presented in **Table 1**.

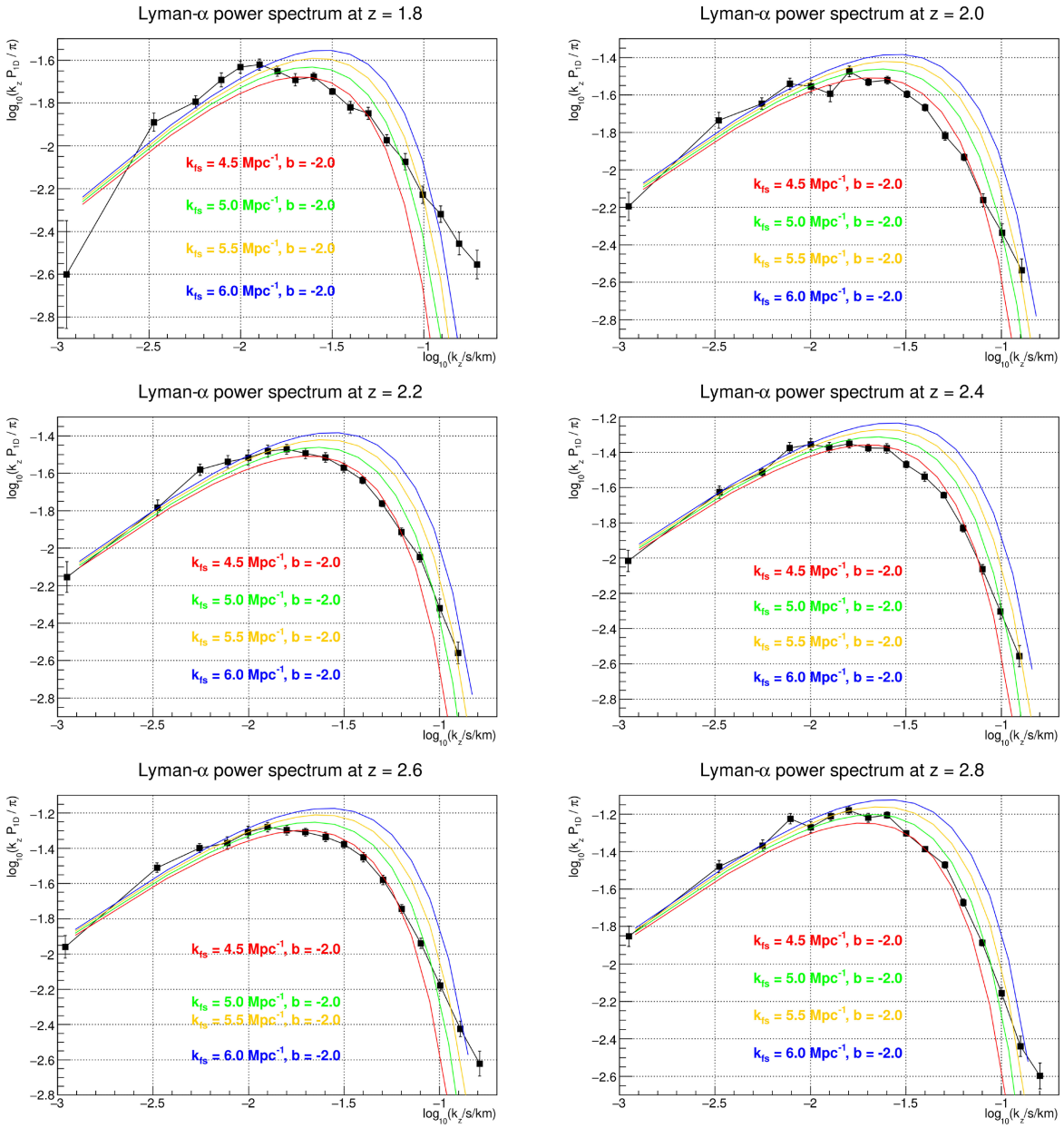

Figure 1. Lyman-α power spectra from [5] in redshift bins $z = 1.8$ to 2.8. k_z is the line-of-sight wavevector in units s/km. $P_{1D}(k_z)$ is the 1-dimensional Lyman-α flux power spectrum. $k_z P_{1D}(k_z)/\pi$ is the dimensionless power spectrum. The Lyman-α flux is measured in bins of wavelength λ. k_z is defined as $k_z \equiv 2\pi/\Delta v$ with $\Delta v \equiv c(\lambda - \lambda_{ref})/\lambda_{ref}$. The reference λ_{ref} is unspecified. The calculated curves are explained in Section 3.

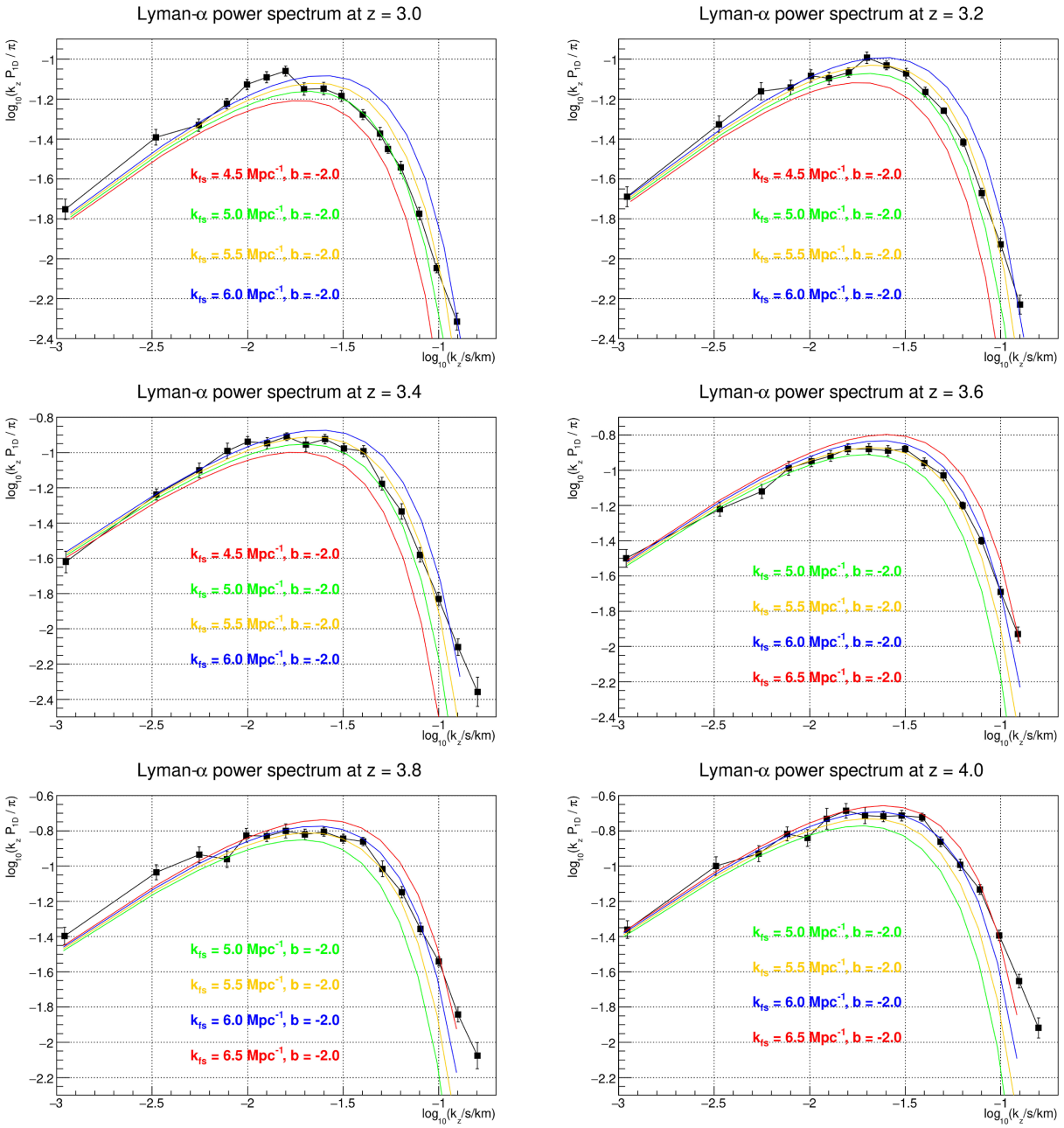

Figure 2. Same as **Figure 1** for redshift bins $z = 3.0$ to 4.0.

To understand **Figures 1-3**, let us mention that Lyman-α flux measurements are made in wavelength bins. The Lyman-α power spectrum $P_{\mathrm{1D}}(k_z)$ is expressed as a function of the wavevector $k_z \equiv 2\pi/\Delta v$, defined in terms of the radial "velocity" $\Delta v \equiv c(\lambda - \lambda_{\mathrm{ref}})/\lambda_{\mathrm{ref}}$. λ_{ref} is unspecified (it usually corresponds to $\lambda_{\mathrm{ref}} = \lambda_\alpha(1+z)$ with z at the center of the redshift bin, or the quasar z). The comoving wavevector k of the comoving density power spectrum $P_{\mathrm{3D}}(k)$ is expressed in units of inverse comoving distance, e.g. Mpc^{-1}, while k_z is expressed in inverse velocity units, e.g. s/km. The conversion factor for the radial wavevector k_z in units s/km to radial Mpc^{-1}, for one bin of a_i, is $H_i a_i$, where

$a_i = 1/(1+z_i)$ is the expansion parameter corresponding to the observed neutral hydrogen "cloud", and $H_i \equiv (\mathrm{d}a_i/\mathrm{d}t)/a_i = H_0\sqrt{\Omega_m/a_i^3 + \Omega_\Lambda}$ is the Hubble parameter at a_i. This conversion factor can be understood as follows: H_i^{-1} converts the radial velocity of an H_I atom at a_i to an equivalent proper radial distance of an expanding "cloud" at a_i, and the factor $1/a_i$ converts this proper radial distance to the corresponding comoving distance. For details, see derivations in **Appendix A** and **Appendix B**. Note that the conversion factor depends on the "cloud" expansion parameter a_i.

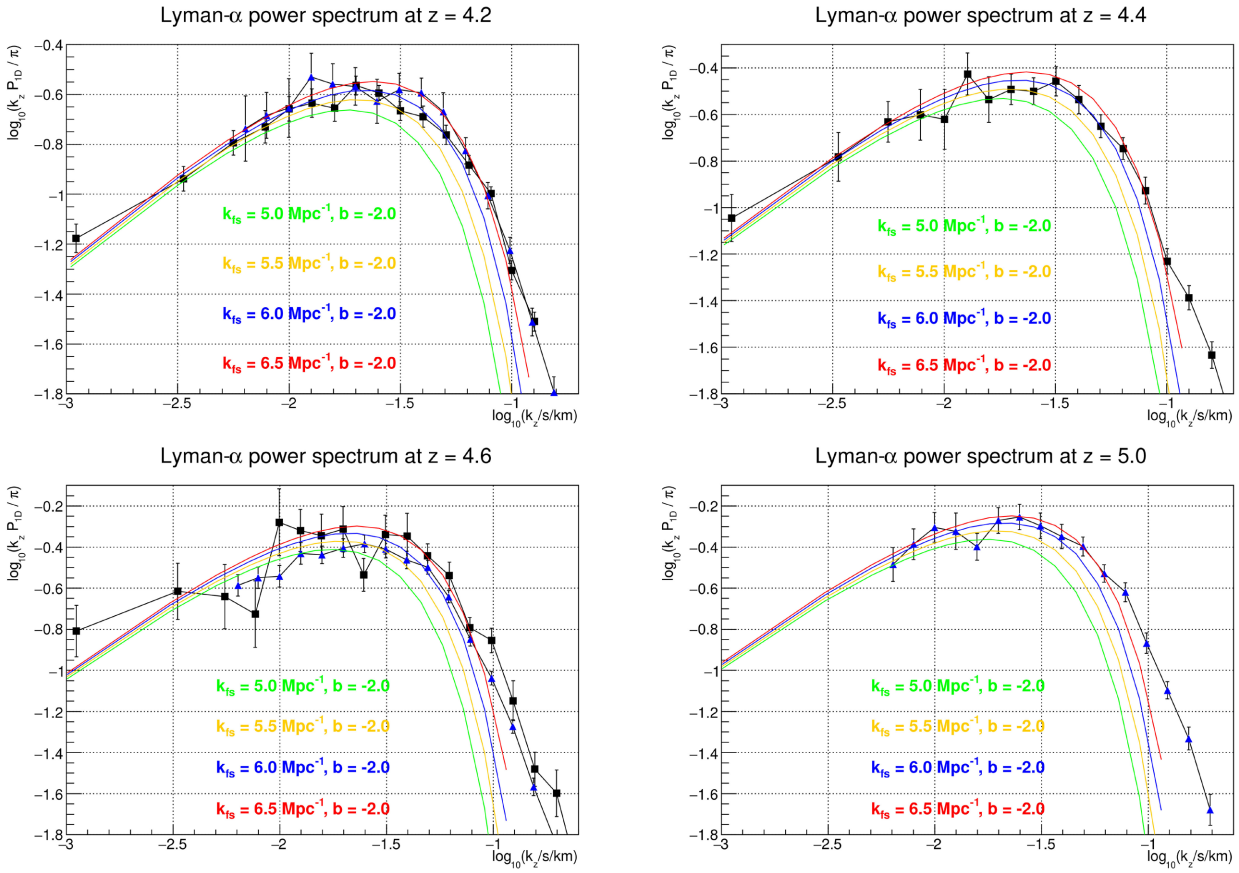

Figure 3. Same as **Figure 1** for redshift bins $z = 4.2$ to 5.0. Power spectra from [5] (black squares) and [14] (blue triangles).

Table 1. At each redshift z are presented k_{fs} and $AB/(1+z)^4$ (defined in (1)-(3)), obtained from **Figures 1-3**. Their uncertainties are ±0.3 Mpc^{-1} and ±0.002 km·s^{-1}·Mpc^2, respectively. These uncertainties include statistical uncertainties and uncertainties from the fit qualities. We note that AB is approximately $\propto (1+z)^4$ so we present $AB/(1+z)^4$.

z	1.8	2.0	2.2	2.4	2.6	2.8	3.0	3.2
k_{fs} [Mpc^{-1}]	4.5	4.3	4.3	4.3	4.5	4.5	4.8	5.1
$AB/(1+z)^4$ [km·s^{-1}·Mpc^2]	0.012	0.013	0.010	0.011	0.010	0.009	0.008	0.009
z	3.4	3.6	3.8	4.0	4.2	4.4	4.6	5.0
k_{fs} [Mpc^{-1}]	5.0	5.6	5.7	5.7	6.4	6.6	6.4	6.7
$AB/(1+z)^4$ [km·s^{-1}·Mpc^2]	0.009	0.009	0.008	0.008	0.009	0.011	0.012	0.010

Why does the observed Lyman-α power spectrum $P_{1D}(k_z)$, presented in Figures 1-3, have a cut-off? We consider two alternatives: i) the density power spectrum cut-off due to warm dark matter free-streaming in the early universe, or ii) the neutral hydrogen H_I thermal velocity Doppler shift.

3. Dark Matter Warmness

Let us assume that the dark matter cut-off wavevector k_{fs} (defined below) is the only source of the Lyman-α power spectrum $P_{1D}(k_z)$ cut-off. For comparison with the data, continuous lines in Figures 1-3 present Lyman-α forest power spectra $P_{1D}(k_z)$ calculated from the 3-dimensional comoving density power spectrum $P_{3D}(k)$ as follows:

$$P_{1D}(k_z) = \frac{B}{2\pi}\int_{k_z}^{\infty} P_{3D}(k)\,k\mathrm{d}k, \tag{1}$$

with $P_{3D}(k)$ approximated by (see Figure 22.5 of [15])

$$P_{3D}(k) = A\left(\frac{k}{6\ \mathrm{Mpc}^{-1}}\right)^{b} \tau^2(k), \tag{2}$$

with $b = -2$, and with the small-scale cut-off factor approximated to

$$\tau^2(k) = \exp\left(-\frac{k^2}{k_{fs}^2}\right). \tag{3}$$

These equations define k_{fs}, A, B and b. Note that this is our definition of the comoving cut-off wavevector k_{fs}: $\tau^2(k_{fs}) = 1/e$. (Alternative definitions in the literature are $\tau^2(k_{fs}) = 1/2$ or 1/4.) As shown in Figures 1-3, the adopted exponential $\tau^2(k)$ is in quite good agreement with the data for $z > 2.2$. We do not understand the disagreements for $z \le 2.0$. For a dimensionless Lyman-α power spectrum $k_z P_{1D}(k_z)/\pi$, AB has units km·s^{-1}·Mpc^2. The factor $1/(2\pi)$ in (1) obtains the conventional normalization of B.

In Equation (1), $P_{3D}(k)$ is the comoving 3-dimensional power spectrum of the quasar flux, which we approximate to the comoving 3-dimensional power spectrum of the matter density, an approximation valid in the linear regime [16].

Figures 1-3 and Table 1 present 16 measurements of the comoving wavevector k_{fs} that range from 4.5 ± 0.3 Mpc^{-1} at $z = 1.8$ to 6.7 ± 0.3 Mpc^{-1} at $z = 5.0$. It turns out that these measurements of k_{fs} are in agreement, within uncertainties, with four independent measurements of k_{fs} summarized in Table 3 of [2]. If this interpretation of the observed $P_{1D}(k_z)$ cut-off is correct, the measured k_{fs} should be independent of z. The observed dependence of k_{fs} on z may, or may not, be significant, see Figure 4, so we discuss this issue in Section 6 below. The dependence of the calculations on the slope b is presented in Figure 5.

Let us relate k_{fs} with the warm dark matter comoving root-mean-square free-streaming distance l_{fs}. Consider the 3-dimensional power spectrum of equation (2). It is the square of the Fourier transform of the smoothed density field $\tilde{\rho}(\boldsymbol{x})$. The square root of (2) is the product of two functions, *i.e.* k^{-1} and

$\exp\left[-k^2/\left(2k_{\mathrm{fs}}^2\right)\right]$. The inverse Fourier transform of this product is the convolution of the two inverse Fourier transforms, *i.e.* $\propto \rho(\boldsymbol{x})$ and $\propto \exp\left[-|\boldsymbol{x}|^2 k_{\mathrm{fs}}^2/2\right]$:

$$\tilde{\rho}(\boldsymbol{x}) = \frac{k_{\mathrm{fs}}^3}{(2\pi)^{3/2}} \int_{-\infty}^{+\infty} \rho(\boldsymbol{y}) \exp\left[-\frac{|\boldsymbol{x}-\boldsymbol{y}|^2 k_{\mathrm{fs}}^2}{2}\right] \mathrm{d}^3\boldsymbol{y}. \tag{4}$$

(For convenience, Fourier transforms of gaussians are presented in **Appendix C**.) Note that this convolution obtains the weighted average of $\rho(\boldsymbol{x})$ over a comoving 3-dimensional root-mean-square distance that is proportianal to l_{fs}: $l_{\mathrm{fs}} \approx 1.31/k_{\mathrm{fs}}$, see (27) of [1]. (The relation is approximate: it depends on the distribution of velocities of the dark matter particles [1].)

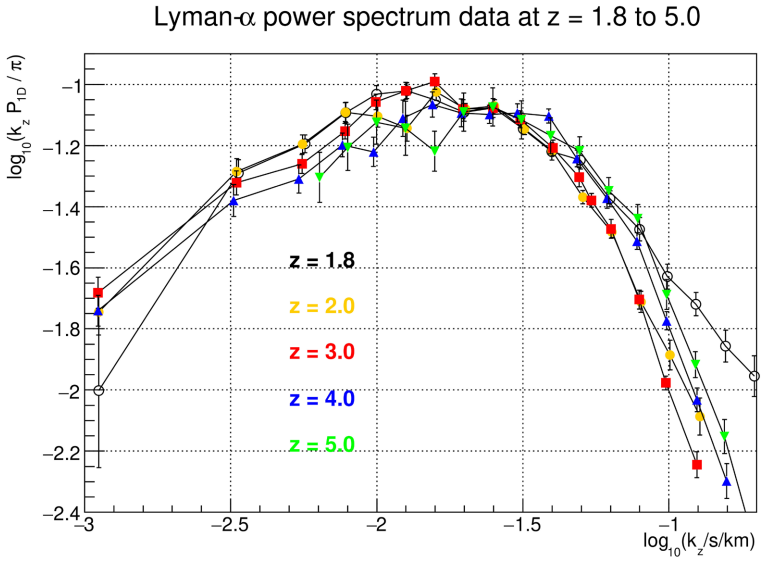

Figure 4. Observed Lyman-α power spectra [5] [14] at $z = 1.8$ to $z = 5.0$. Amplitudes have been adjusted so that all $k_z P_{1\mathrm{D}}(k_z)/\pi$ coincide at $\log_{10}(k_z/\mathrm{s/km}) = -1.7$.

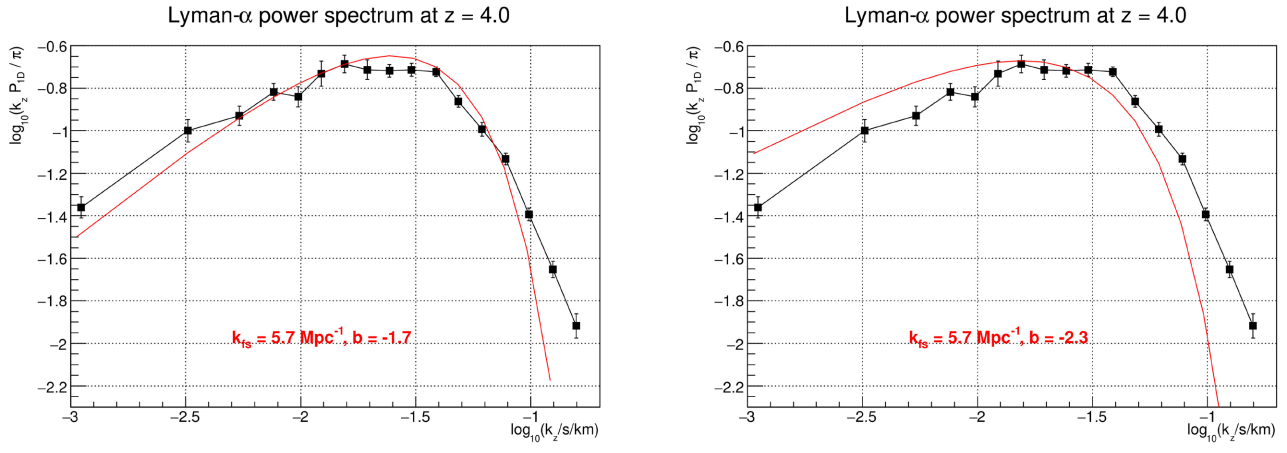

Figure 5. The observed Lyman-α power spectrum [5] at $z = 4.0$ is compared with calculation for $k_{\mathrm{fs}} = 5.7$ Mpc^{-1}, and $b = -1.7$ and $b = -2.3$ (red lines). For $b = -2.0$, see **Figure 2**.

Consider a quasar flux as a function of $v \equiv c\Delta\lambda/\lambda$. An absorption from an iso-

lated "cloud" has the form $\exp\left[-\left(v-v_0\right)^2/\left(2\sigma^2\right)\right]$. If the cloud has temperature T and is small, or non-expanding, the root-mean-square velocity of the neutral hydrogen atoms along the line-of-sight is $\sigma=\sqrt{k_{\mathrm{B}}T/m_p}$. If the cloud is cold and has a comoving root-mean-square length $l_{\mathrm{fs}}/\sqrt{3}$ along the line-of-sight, and is expanding, then the proper root-mean-square thermal velocity along the line-of-sight is $\sigma=l_{\mathrm{fs}}a_iH_i/\sqrt{3}$. If the cloud is both hot and expanding, then $\sigma=\sqrt{\left(k_{\mathrm{B}}T/m_p\right)+\left(l_{\mathrm{fs}}a_iH_i\right)^2/3}$.

We may relate l_{fs} to an equivalent temperature of a hydrogen "cloud" observed at expansion parameter a_i:

$$T=\frac{m_p\left(l_{\mathrm{fs}}a_iH_i\right)^2}{3k_{\mathrm{B}}}\approx 0.57\frac{m_p\left(a_iH_i\right)^2}{k_{\mathrm{B}}k_{\mathrm{fs}}^2}. \tag{5}$$

Note that T and k_{fs} are degenerate, *i.e.* they can not be individually measured with Lyman-α forest data alone (assuming that both non-relativistic dark matter particles and neutral hydrogen atoms have the same thermal Maxwell velocity distribution). (Note that published limits on k_{fs}, or the warm dark matter thermal relic mass, obtained solely with Lyman-α forest data, need to be taken with caution.) Our major challenge is to distinguish warm dark matter from hot neutral hydrogen, with data *independent* of the Lyman-α forest.

4. HI Temperature

In Section 3, we assume that warm dark matter is the only cause of the observed Lyman-α forest power spectrum cut-off, implying that the intergalactic baryons are relatively cold. In this section we consider the opposite case: the baryon temperature is the only cause of the observed Lyman-α power spectrum cut-off, while dark matter is cold. There are several thermal effects. In this section we only consider the leading and simplest one, namely the neutral hydrogen thermal velocity Doppler shift. It is important to realize that, as long as the universe expands linearly, $\Delta v\equiv c\Delta\lambda/\lambda$ is independent of $a(t)$.

From (5), for $z=5,4$ and 2, and k_{fs} from **Table 1**, we obtain the needed temperature to cause the observed Lyman-α flux power spectrum cut-off assuming cold dark matter: $T\approx 13000$ K, 15,000 K and 16,000 K, respectively. In summary, if $T\approx 15000$ K, then the Lyman-α flux power spectrum cut-off is due to temperature alone, and the data is consistent with the cold dark matter ΛCDM scenario. On the other hand, if $T\lesssim 15000$ K, then the cut-off requires warm dark matter free-streaming.

The mean temperature, at mean density, obtained from Lyman-α data and simulations that assume the cold dark matter ΛCDM scenario is approximately $T\approx 10000$ K [17]-[21]. The width of Lyman-α absorption features depend on the integalactic baryon temperature, and is compared with simulations to constrain the temperature [19]. However, this width is degenerate with the dark matter warmness.

At redshif $z\lesssim 6$ the intergalactic medium is highly ionized. The temperature

of the intergalactic medium at redshift $z = 4$ is highly variable, from ≈ 2000 K in underdense regions, to ≈ 10^6 K in highly dense shock-heated gas. What is the temperature of the neutral hydrogen "clouds" (without using Lyman-α forest data assuming cold dark matter)? We do not know, see Section 7.

5. Amplitude of $P_{1D}(k_z)$

AB, defined in (1)-(3), is expected to scale as $AB \propto (1+z)^{-2}(n_{HI}/n_H)(1+z)^3$. The first factor is due to the scaling of $P_{3D}(k)$, and the last factor is due to density (to compensate the ionized plus neutral hydrogen density n_H). The fraction of neutral hydrogen n_{HI}/n_H at low n_H scales in proportion to density [22], *i.e.* $\propto (1+z)^3$, because of the mean-free-path for the reaction $p^+ + e^- \to H_1$. The observed dependence of AB on z is $AB \propto (1+z)^4$, see Table 1, so the dependence of AB on z is understood, at least in first approximation.

6. Comments on the Possible Dependence of the Observed k_{fs} on z

If the cut-off of $P_{1D}(k_z)$ is due only to dark matter free-streaming, we expect k_{fs} to be approximately independent of z (because free-streaming is only effective in the early universe at expansion parameter of order $a_{eq} \approx 1/3402$). However, the observed k_{fs} decreases from 6.4 ± 0.3 to 4.3 ± 0.3 from $z = 4.6$ to $z = 2.0$. The significance of the dependence of k_{fs} on z may also be judged from Figure 4. What is the cause of this possible dependence?

- The large variation of the amplitude AB from $z = 5.0$ to 1.8 may result in an unknown experimental systematic dependence of the observed k_{fs} on z.
- If warm dark matter free-streaming is the only cause of the observed $P_{1D}(k_z)$ cut-off, we expect no dependence of k_{fs} on z so long as the density is linear and the universe is expanding homogeneously. However, a dependence of the observed k_{fs} on z will set in when density perturbations become non-linear. Consider an overdense region of the universe that expands slower than a. The density peaks attract each other resulting in an *increase* of the observed comoving k_{fs}. Some peaks coaless resulting in the bottom-up hierachical evolution of the density fluctuations, and a *reduction* of the observed k_{fs}.
- Equations (1)-(3) are approximate: they assume that the neutral hydrogen density is proportional to the matter density, an approximation valid if density perturbations are linear. Non-linear density perturbations will introduce corrections to equations (1)-(3).
- The conversion factor $H_i a_i$ becomes approximate when density perturbations become non-linear.
- Perhaps intergalactic thermal velocity Doppler shift of neutral hydrogen, or Jeans smoothing, compete with warm dark matter free-streaming.
- Note that the zero point of Δv is not specified: we have assumed $\lambda_{ref} = \lambda_\alpha (1+z)$, with z at the mid-point of the redshift bin.

7. Trying to Break the Degeneracy

The Lyman-α forest power spectrum has an observed cut-off that may be due to warm dark matter free-streaming or to the intergalactic neutral hydrogen temperature. The Lyman-α forest data apparently can not distinguish between these two alternatives. Which of these alternatives is dominant? One way to break this degeneracy is to estimate the intergalactic baryon temperature, as a function of mean hydrogen (ionized plus neutral) number density, based on the measured ultra-violet intensity. A summary of four calculations ([23]-[26]) can be found in [22]. From Figure 1 of [22] we obtain the temperatures listed in **Table 2**. From the large temperature uncertainties, we are unable to lift the degeneracy.

Alternative ways to break the degeneracy are measurements of the dark matter k_{fs} without the Lyman-α forest. Four independent measurements of k_{fs} are presented in Table 3 of [2] (and references therein), that are in agreement with **Table 1**, but in disagreement, by a factor of order few, with limits summarized in Table 3 of [3]. Note that each of these measurements and limits have their own issues.

In summary, we are unable to clearly favor one or the other alternative. Perhaps both warm dark matter and baryon temperature contribute to the observed Lyman-α power spectrum cut-off?

Table 2. For redshifts $z=5$ and $z=2$, are presented the mean hydrogen (neutral plus ionized) number density $\langle n_{\text{H}}\rangle = \Omega_b \rho_{\text{crit}} (1+z)^3 / m_p$, and the corresponding calculated temperatures from the measured UV intensity [22].

z	$\langle n_{\text{H}}\rangle$ [cm^{-3}]	T [K]
5	5.4×10^{-5}	$\approx 10^{2}$ to $10^{5.5}$
2	6.8×10^{-6}	$\approx 10^{1}$ to $10^{5.0}$

8. Both?

There are two total (dark matter plus baryon) masses of interest: the half-mode mass M_{hm} and the Jeans mass M_{J} [1]. M_{hm} depends on the warm dark matter cut-off wavevector k_{fs}, and the Jeans mass M_{J} depends on the hydrogen temperature T [1] [27]. The two masses are equal if

$$\left(\frac{k_{\text{fs}}}{5.7\ \text{Mpc}^{-1}}\right)^2 = \frac{1+z}{1+4}\frac{12000\ \text{K}}{T}. \tag{6}$$

If $M_{\text{hm}} \gg M_{\text{J}}$, *i.e.* dark matter is sufficiently warm, then M_{hm} is the smallest clump of total (dark matter plus baryon) mass that will collapse due to its own gravity, and this collapse includes the full complement of baryons. In this case there is no Jeans smoothing. If $M_{\text{hm}} \ll M_{\text{J}}$, *i.e.* baryons are sufficiently hot, then clumps of total matter with mass greater than M_{hm}, and less than M_{J}, will have dark matter collapsing but without the full complement of baryons.

Before $z \approx 150$, hydrogen is in thermal equilibrium with the cosmic microwave background radiation, and the total (dark matter plus baryon)

$M_{\mathrm{J}} \approx 6\times10^{5} M_{\odot}$ [27]. After reionization, the temperature jumps to ≈12,000 K and M_{J} jumps to $\approx 10^{10} M_{\odot}$. Let us now consider the two scenarios.

If dark matter is warm: Assume $M_{\mathrm{hm}} > M_{\mathrm{J}}$. To be specific consider $z \approx 4$, $k_{\mathrm{fs}} \approx 5.7$ Mpc^{-1} and $T \lesssim 12000$ K after reionization. In this case $M_{\mathrm{hm}} \approx 10^{10} M_{\odot}$ [1]. First density perturbations to collapse have comoving wavevector k of order k_{fs}, and ride on top of larger and larger perturbations that have similar phases and so add up. The relative amplitudes of these perturbations grow in proportion to the expansion parameter $a(t)$ while linear. First clumps of mass to collapse have total (dark matter plus baryon) mass of order $\approx M_{\mathrm{hm}}/10 \approx 10^{9} M_{\odot}$ (taking into account the tail of $P_{3\mathrm{D}}(k)$). Galaxy formation is hierarchical, from bottom-up, starting at mass of order $10^{9} M_{\odot}$, due to larger and larger perturbations becoming non-linear, resulting in the merging of galaxy halos; and also hierarchical formation from top-down, starting at mass of order $10^{9} M_{\odot}$, due to halos loosing mass to neighboring halos. The corresponding dwarf galaxies do not have time to desintegrate due to the low dark matter particle velocities ($\approx (1+z)\times 120$ m/s). Is there any evidence for this scenario? Yes! I refer the reader to Section 4 of [2].

Equation (6) is extraordinary: is it a coincidence, or is it telling us something? Equation (6) relates two minimum total (dark matter plus baryon) mass clumps that can collapse: M_{hm} depending on the dark matter temperature-to-mass ratio, and M_{J} depending on baryon temperature. The first generation of stars emit ultra-violet radiation that heat up and ionize the intergalactic hydrogen atoms. Let us speculate that, when the temperature reaches of order 12,000 K, during reionization, collapsing halos begin loosing their baryons, and the formation of stars is inhibeted, so the temperature approaches an equilibrium value. (Hot baryons also directly inhibit star formation, but such inhibition is not addressed by Equation (6).) Equation (6) is, perhaps, not a coincidence! It is perhaps telling us that the intergalactic temperature after reionization is self-regulating. Note that k_{fs} in Equation (6) is the warm dark matter power spectrum cut-off wavevector, and has no relation to the neutral hydrogen thermal velocity Doppler shift. Note also that Equation (6) is in agreement with observations. If (6) is not a coincidence, it is telling us that dark matter is warm!

Another sealing to the baryon temperature is $T \approx 10000$ K to 4000 K due to hydrogen excitation followed by decay and radiation, see Figure 7 of [28].

If dark matter is cold: Assume dark matter is very cold, *i.e.* $k_{\mathrm{fs}} \gtrsim 170$ Mpc^{-1}. Then first perturbations to collapse, before reionization, have dark matter mass smaller than $6\times10^{5} M_{\odot}$ and are nearly free of baryons. The collapse of matter is hierarchical, bottom-up. The first halos that collapse with the full complement of bayons, before reionization, have total (dark matter plus baryon) mass or order $6\times10^{5} M_{\odot}$. At this point first stars begin forming, ionizing and heating up the baryons. Is an equilibrium reached?

9. Summary

Data that favor warm dark matter:

- Galaxies apparently form hierarchically, starting at $\approx 10^9 M_\odot$, bottom-up and top-down, see Section 4 of [2] and references therein.
- Four independent measurements of $k_{\rm fs}$ are in agreement with the warm dark matter Lyman-α power spectrum cut-off, see Table 3 of [2].

Data that favor cold dark matter:

- Limits on warm dark matter summarized in Figure 3 of [3]. (Limits that depend only on Lyman-α forest data need to be taken with caution, see Section 3.)
- The possible dependence of the measured $k_{\rm fs}$ on z, see Section 3.

10. Conclusions

The Lyman-α forest flux power spectrum $P_{\rm 1D}(k_z)$ has an observed cut-off. This cut-off may be due to warm dark matter free-streaming in the early universe, or to hot baryons, or both. These degenerate alternatives can not be distinguished with Lyman-α flux spectra alone. Limits on $k_{\rm fs}$ obtained with Lyman-α data alone need to be taken with caution. Data favoring warm or cold dark matter are summarized in Section 9. If warm dark matter is the leading effect, *i.e.* if $T \lesssim 10000$ K, we obtain

$$k_{\rm fs} = 5.7 \pm 0.3 \pm 2.0 \text{ Mpc}^{-1}. \tag{7}$$

The first uncertainty is due to statistical uncertainties of the measured power spectra and the quality of the fits, and the second uncertainty is estimated from "other" phenomena listed in Section 6, the dispersion of measurements in **Figure 4**, and the apparent dependence of $k_{\rm fs}$ on redshift z in **Table 1**. This result is in agreement with [2] and [1], but in disagreement with measurements summarized in Figure 3 of [3]. A comparison of the present analysis and a limit obtained with the Lyman-α forest [4] is presented in **Appendix D**.

Conflicts of Interest

The author declares no conflicts of interest regarding the publication of this paper.

References

[1] Hoeneisen, B. (2026) Study of Warm Dark Matter with the Lyman-α Forest. *International Journal of Astronomy and Astrophysics*, **16**, 145-160. https://doi.org/10.4236/ijaa.2026.163010

[2] Hoeneisen, B. (2026) Update to Four Estimates of the Dark Matter Warmness. *International Journal of Astronomy and Astrophysics*, **16**, 79-93. https://doi.org/10.4236/ijaa.2026.162006

[3] Liu, B., Shan, H. and Zhang, J. (2024) New Galaxy UV Luminosity Constraints on Warm Dark Matter from JWST. *The Astrophysical Journal*, **968**, Article 79. https://doi.org/10.3847/1538-4357/ad4ed8

[4] Iršič, V., Viel, M., Haehnelt, M.G., Bolton, J.S., Molaro, M., Puchwein, E., *et al.* (2024) Unveiling Dark Matter Free Streaming at the Smallest Scales with the High Redshift Lyman-Alpha Forest. *Physical Review D*, **109**, Article 043511. https://doi.org/10.1103/physrevd.109.043511

[5] Karaçaylı, N.G., Padmanabhan, N., Font-Ribera, A., Iršič, V., Walther, M., Brooks, D., *et al.* (2022) Optimal 1D Ly A Forest Power Spectrum Estimation—II. KODIAQ, SQUAD, and XQ-100. *Monthly Notices of the Royal Astronomical Society*, **509**, 2842-2855. https://doi.org/10.1093/mnras/stab3201

[6] Lehner, N., O'Meara, J.M., Fox, A.J., Howk, J.C., Prochaska, J.X., Burns, V. and Armstrong, A.A. (2017) The Second Data Release of the KODIAQ Survey. *The Astrophysical Journal*, **154**, Article 114.

[7] O'Meara, J.M., Lehner, N., Howk, J.C., Prochaska, J.X., Fox, A.J., Swain, M.A., *et al.* (2015) The First Data Release of the Kodiaq Survey. *The Astronomical Journal*, **150**, Article 111. https://doi.org/10.1088/0004-6256/150/4/111

[8] O'Meara, J.M., Lehner, N., Howk, J.C., Prochaska, J.X., Fox, A.J., Peeples, M.S., *et al.* (2017) The Second Data Release of the KODIAQ Survey. *The Astronomical Journal*, **154**, Article 114. https://doi.org/10.3847/1538-3881/aa82b8

[9] Vogt, S.S., Allen, S.L., Bigelow, B.C., Bresee, L., Brown, B., Cantrall, T., Conrad, A., Couture, M., *et al.* (1994) HIRES: The High-Resolution Echelle Spectrometer on the Keck 10-M Telescope. In: Crawford, D.L. and Craine, E.R., Eds., *Instrumentation in Astronomy VIII*, SPIE, 362-375

[10] Murphy, M.T., Kacprzak, G.G., Savorgnan, G.A.D. and Carswell, R.F. (2019) The UVES Spectral Quasar Absorption Database (SQUAD) Data Release 1: The First 10 Million Seconds. *Monthly Notices of the Royal Astronomical Society*, **482**, 3458-3479. https://doi.org/10.1093/mnras/sty2834

[11] Dekker, H., D'Odorico, S., Kaufer, A., Delabre, B. and Kotzlowski, H. (2000) Design, Construction, and Performance of UVES, the Echelle Spectrograph for the UT2 Kueyen Telescope at the ESO Paranal Observatory. *SPIE Proceedings*, **4008**, 534-545. https://doi.org/10.1117/12.395512

[12] Vernet, J., Dekker, H., D'Odorico, S., Kaper, L., Kjaergaard, P., Hammer, F., *et al.* (2011) X-Shooter, the New Wide Band Intermediate Resolution Spectrograph at the ESO Very Large Telescope. *Astronomy & Astrophysics*, **536**, A105. https://doi.org/10.1051/0004-6361/201117752

[13] López, S., D'Odorico, V., Ellison, S.L., Becker, G.D., Christensen, L., Cupani, G., *et al.* (2016) XQ-100: A Legacy Survey of One Hundred $3.5 \lesssim z \lesssim 4.5$ Quasars Observed with VLT/X-Shooter. *Astronomy & Astrophysics*, **594**, A91. https://doi.org/10.1051/0004-6361/201628161

[14] Boera, E., Becker, G.D., Bolton, J.S. and Nasir, F. (2019) Revealing Reionization with the Thermal History of the Intergalactic Medium: New Constraints from the Lyα Flux Power Spectrum. *The Astrophysical Journal*, **872**, Article 101. https://doi.org/10.3847/1538-4357/aafee4

[15] Takahashi, F., *et al.* (2026) The Review of Particle Physics (2026) *International Journal of Modern Physics A*, **41**, Article 2630011.

[16] Niemeyer, J.C. (2020) Small-Scale Structure of Fuzzy and Axion-Like Dark Matter. *Progress in Particle and Nuclear Physics*, **113**, Article 103787. https://doi.org/10.1016/j.ppnp.2020.103787

[17] D'Aloisio, A., McQuinn, M., Maupin, O., Davies, F.B., Trac, H., Fuller, S., *et al.* (2019) Heating of the Intergalactic Medium by Hydrogen Reionization. *The Astrophysical Journal*, **874**, Article 154. https://doi.org/10.3847/1538-4357/ab0d83

[18] Hu, T., Khaire, V., Hennawi, J.F., Tripp, T.M., Oñorbe, J., Walther, M., *et al.* (2025) Measurements of the Thermal and Ionization State of the Intergalactic Medium during the Cosmic Afternoon. *Monthly Notices of the Royal Astronomical Society*, **536**, 1-26. https://doi.org/10.1093/mnras/stae2474

[19] Becker, G.D., Bolton, J.S., Haehnelt, M.G. and Sargent, W.L.W. (2010) Detection of Extended He II Reionization in the Temperature Evolution of the Intergalactic Medium. *Monthly Notices of the Royal Astronomical Society*, **410**, 1096-1112. https://doi.org/10.1111/j.1365-2966.2010.17507.x

[20] Gaikwad, P., Srianand, R., Haehnelt, M.G. and Choudhury, T.R. (2021) A Consistent and Robust Measurement of the Thermal State of the IGM at $2 \le z \le 4$ from a Large Sample of Ly α Forest Spectra: Evidence for Late and Rapid He ii Reionization. *Monthly Notices of the Royal Astronomical Society*, **506**, 4389-4412. https://doi.org/10.1093/mnras/stab2017

[21] Bolton, J.S., Becker, G.D., Haehnelt, M.G. and Viel, M. (2014) A Consistent Determination of the Temperature of the Intergalactic Medium at Redshift $\langle z \rangle = 2.4$. *Monthly Notices of the Royal Astronomical Society*, **438**, 2499-2507. https://doi.org/10.1093/mnras/stt2374

[22] Taira, E., Kopenhafer, C. and O'Shea, B.W. (2025) Metagalactic Ultraviolet Background Tables for Calculating Diffuse Astrophysical Plasma Properties. *Research Notes of the AAS*, **9**, Article 129. https://doi.org/10.3847/2515-5172/adddae

[23] Faucher-Giguère, C., Lidz, A., Zaldarriaga, M. and Hernquist, L. (2009) A New Calculation of the Ionizing Background Spectrum and the Effects of He II Reionization. *The Astrophysical Journal*, **703**, 1416-1443. https://doi.org/10.1088/0004-637x/703/2/1416

[24] Haardt, F. and Madau, P. (2012) Radiative Transfer in a Clumpy Universe. IV. New Synthesis Models of the Cosmic UV/X-Ray Background. *The Astrophysical Journal*, **746**, Article 125. https://doi.org/10.1088/0004-637x/746/2/125

[25] Puchwein, E., Haardt, F., Haehnelt, M.G. and Madau, P. (2019) Consistent Modelling of the Meta-Galactic UV Background and the Thermal/Ionization History of the Intergalactic Medium. *Monthly Notices of the Royal Astronomical Society*, **485**, 47-68. https://doi.org/10.1093/mnras/stz222

[26] Faucher-Giguère, C. (2020) A Cosmic UV/X-Ray Background Model Update. *Monthly Notices of the Royal Astronomical Society*, **493**, 1614-1632. https://doi.org/10.1093/mnras/staa302

[27] Weinberg, S. (2008) Cosmology. Oxford University Press.

[28] Inayoshi, K., Visbal, E. and Haiman, Z. (2020) The Assembly of the First Massive Black Holes. *Annual Review of Astronomy and Astrophysics*, **58**, 27-97. https://doi.org/10.1146/annurev-astro-120419-014455

Appendix

A. Lyman-α Absorption

We consider pulses of light propagating radialy in a flat universe. The metric is $\mathrm{d}s^2 = c^2\mathrm{d}t^2 - a(t)^2\,\mathrm{d}r^2$. Note that the radial coordinate r is the present, or comoving, distance to an event. For simplicity, we neglect the cosmological constant in these appendices. Then the evolution of the homogeneous universe is described by

$$H \equiv \frac{\mathrm{d}a/\mathrm{d}t}{a} = H_0\sqrt{\frac{\Omega_m}{a^3}}, \tag{8}$$

$$\frac{2}{3}a^{3/2} = H_0\sqrt{\Omega_m}\,t. \tag{9}$$

Consider a neutral hydrogen "cloud" that absorbes Lyman-α photons at the proper wavelength $\lambda_i = 1215.67$ Å, and at the expansion parameter a_i. The universal time of the absorption is

$$t_i = \frac{2}{3H_0\sqrt{\Omega_m}}a_i^{3/2}, \tag{10}$$

and the present day, or comoving, distance to the "cloud" is

$$r_i = \frac{2c}{H_0\sqrt{\Omega_m}}\left(a_f^{1/2} - a_i^{1/2}\right). \tag{11}$$

This absorption is observed at $r_f = 0$, and the present expansion parameter $a_f = 1$, at the universal time of observation

$$t_f = \left\{t_i^{1/3} + \frac{r_i}{3c}\left(\frac{3H_0\sqrt{\Omega_m}}{2}\right)^{2/3}\right\}^3. \tag{12}$$

Note that the redshifted wavelength λ_f is

$$\frac{\partial t_f}{\partial t_i} = \frac{\lambda_f}{\lambda_i} = \frac{a_f}{a_i}. \tag{13}$$

B. Conversion from Comoving Radial Distance Δr to Radial "Velocity" $\Delta v \equiv c\Delta\lambda/\lambda$

(For simplicity we consider a homogeneous flat universe and neglect the cosmological constant.) Consider two Lyman-α lines from two "clouds" at r_i and $r_i + \Delta r$. The received wavelength at the origin at the universal time t is $\lambda_\alpha/a(t)$ for both clouds. We would like to compare the received wavelengths at the same arrival time

$$t_f = \left\{(t_i + \Delta t)^{1/3} + \frac{r_i + \Delta r}{3c}\left(\frac{3H_0\sqrt{\Omega_m}}{2}\right)^{2/3}\right\}^3, \tag{14}$$

so $\Delta t = -\Delta r a_i/c$.

$$a(t+\Delta t) = a(t) + \frac{\mathrm{d}a}{\mathrm{d}t}\Delta t = a_i\left(1+\frac{2}{3t_i}\Delta t\right), \tag{15}$$

$$\lambda_i = \frac{\lambda_\alpha}{a_i};\ \lambda_i' = \frac{\lambda_\alpha}{a_i'} = \frac{\lambda_\alpha}{a_i}\left(1-\frac{2}{3t_i}\Delta t\right), \tag{16}$$

$$\Delta v \equiv c\frac{\lambda_i'-\lambda_i}{\lambda_i} = -c\frac{2}{3t_i}\Delta t = -\Delta r\frac{2a_i}{3t_i}. \tag{17}$$

Note that Δv is a radial "velocity". The last fraction is the conversion factor of interest:

$$\frac{2a_i}{3t_i} = a_i H_0\sqrt{\frac{\Omega_m}{a_i^3}} \equiv a_i H_i. \tag{18}$$

Note that the conversion depends on a_i.

An alternative derivation is as follows: calculate $\mathrm{d}r_i$ from (11) and compare with $\mathrm{d}v$.

C. 1D and 3D Gaussians

The following equations at hand are useful to understand the main text. Consider this normalized 1D Gaussian with standard deviation (or root-mean-square) σ:

$$f(x) = \frac{1}{\sqrt{2\pi}\sigma}\exp\left(-\frac{x^2}{2\sigma^2}\right). \tag{19}$$

Its Fourier transform is

$$F(k) \propto \exp\left(-\frac{k^2\sigma^2}{2}\right). \tag{20}$$

Consider this normalized 3D Gaussian:

$$f(\boldsymbol{x}) = f(|\boldsymbol{x}|) = \frac{1}{(2\pi)^{3/2}\sigma^3}\exp\left(-\frac{|\boldsymbol{x}|^2}{2\sigma^2}\right). \tag{21}$$

Its fourier transform is

$$F(\boldsymbol{k}) = F(|\boldsymbol{k}|) \propto \exp\left(-\frac{k^2\sigma^2}{2}\right). \tag{22}$$

D. Comparison of the Present Analysis with [4]

The present article, Part II, is based on Lyman-α data obtained in [5] and [14]. The article [4] is based on the same data obtained in [14]. Both articles try to understand the observed Lyman-α flux power spectrum cut-off. Both articles should obtain consistent results.

The two articles, Part II and [4], are in approximate agreement. If the baryonic temperature $T \approx 10000$ K [4] or $T \approx 15000$ K (Part II), then the observed cut-off is due to temperature alone, and dark matter is cold. If the temperature is lower, then warm dark matter free-streaming is needed to obtain the observed cut-off. If this is the case, *i.e.* $T \lesssim 10000$ K, the obtained warmness of dark mat-

ter, k_{fs} or equivalently m_{th}, turns out to be in agreement with the measurements summarized in [2] and in [1].

The main difference between Part II and [4] is the external data used to constrain the baryon temperature and break the $T \leftrightarrow k_{\mathrm{fs}}$ degeneracy.